Backward proton production and high-momentum components of nuclei*

H. J. Weber and L. D. Miller
Department of Physics, University of Virginia, Charlottesville, Virginia 22901
(Received 4 April 1977)

The production of energetic protons at 180° by the inclusive reaction $A(p,p')X$ is studied. A mechanism which involves $A-1$ nucleon transfer and relates the inclusive cross section to the total cross section $\sigma_T(p,A-1)$ and realistic nuclear single-particle momentum distributions gives a qualitative understanding of the data.

[NUCLEAR REACTIONS Backward proton production $A(p,p')X$, 600–800 MeV, nuclear single proton distributions (high q) calculated.]

Recently Frankel *et al.*[1] have observed protons of energy $T'_{\rm lab}=0.1$ to 0.4 GeV at 180° lab angle from the collision of $T_{\rm lab}=0.6$ and 0.8 GeV protons with several nuclear targets. Their data for the inclusive reaction $A(p,p')X$ yield beautiful fits (see data in Figs. 1 and 2) of the functional form $d\sigma/d^3p'_{\rm lab} = B_p \exp(-\alpha_p p'^2_{\rm lab}/2m_p)$ where $p'_{\rm lab}$ is the lab momentum of the backward proton. Similar results hold for backward going deuterons and tritons.

In view of the high incident and recoil proton energies involved, a direct reaction mechanism is suggested. For direct reactions the question immediately arises as to whether the backward going proton is the incident proton or one of the constituent protons of the target nucleus. The former seems an unlikely possibility for it would involve either several large angle scatterings from constituent nucleons (all adding up to 180°) or a single 180° scattering, possibly from a point-like quark constituent or one of considerably larger mass than a single nucleon. Thus, Amado and Woloshyn[2] postulate that the reaction proceeds by *forward* scattering of the incident proton from a target proton (or neutron) of momentum q which happens to be traveling opposite to the projectile at the time of collision. This mechanism leads to an inclusive cross section $d\sigma/d^3p'_{\rm lab}$ proportional to the forward proton-nucleon scattering cross section and to the probability $n(q)$ of finding a nucleon of momentum q in the nucleus A.

However, the forward proton-nucleon scattering mechanism is merely one simple extreme of a class of direct reaction mechanisms involving the exchange of ν nucleons where $1\leq\nu\leq A-1$. An equally simple mechanism which also maintains a strong connection with the single-particle momentum distribution is the other extreme, i.e., $A-1$ nucleon exchange.[3] With this mechanism (see insert of Fig. 2) we visualize the target nucleus A splitting into a backward going (observed) proton and an $A-1$ system which then undergoes an inclusive reaction with the incident proton. This mechanism (or an intermediate involving less than $A-1$ nucleon transfer) represents the inclusive nature of the experiment more faithfully than the forward proton-nucleon mechanism which effectively restricts the final $A-1$ system to nuclear one-hole

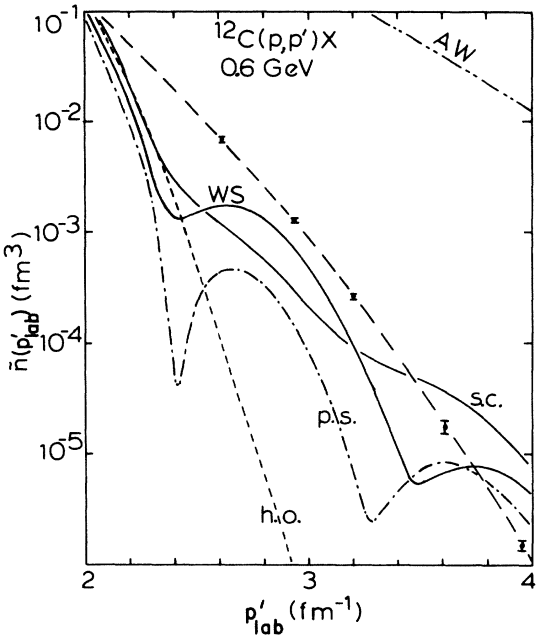

FIG. 1. Nuclear single-proton momentum distributions for ^{12}C. AW is the theoretical parametrization of Amado and Woloshyn. s.c. and WS are theoretical results from the Dirac equation for a self-consistent model (Ref. 8) and a Woods-Saxon well ($V_0=-55.5$ MeV, $R=3.0$ fm, $d=0.5$ fm) used as a scalar potential. The curve denoted p.s. represents the self-consistent calculation with the pair terms suppressed; h.o. is the nonrelativistic harmonic oscillator result with oscillator parameter $b=1.65$ fm. The experimental points, assuming our reaction mechanism, are joined by a smooth dashed curve taken from the parametrization of the data given in Ref. 1.

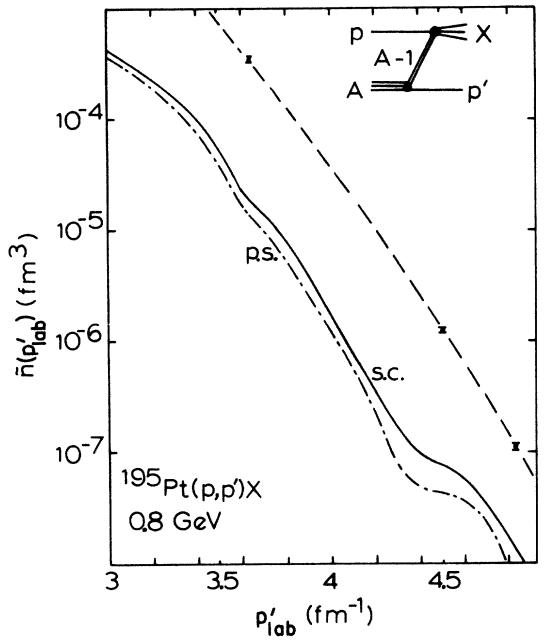

FIG. 2. Nuclear single-proton momentum distributions for ^{195}Pt. The curves denoted p.s. and s.c. result from the self-consistent model both with and without suppression of the pair terms. The experimental points are obtained as in Fig. 1. The inset shows our reaction mechanism.

states when it is taken to involve the nuclear single-particle distribution. In contrast, the inclusive cross section with the $A-1$ nucleon exchange mechanism will be directly proportional to the $(p,A-1)$ total cross section σ_T which involves not only final states with all energetically possible combinations of nucleons but also includes meson production or excited baryon production.

The $A-1$ exchange mechanism leads to the amplitude

$$T=\langle p',A-1\,|\,T_b\,|A\rangle\frac{2m_{A-1}}{Q^2-m_{A-1}^2}\langle X\,|\,T_a\,|A-1,p\rangle \qquad (1)$$

in the lab upon neglecting small off-shell effects for the $(A-1)$ nucleon intermediate state of four-momentum Q. A Wigner-Wick rotation allows us to to write the invariant

$$\sum_{\substack{\text{spins}\\X}}|T|^2=2m_A\bar{n}(p'_{lab})\sum_{\substack{\text{spins}\\X}}|\langle X\,|\,T_a\,|A-1,\tilde{p}\rangle|^2 \qquad (2)$$

in terms of the nuclear single-particle distribution $\bar{n}(p'_{lab})$ in the A rest frame (lab system), where it is normalized to Z protons; $|T_a|^2$ is to be evaluated in the Q rest frame and leads to the total $p-(A-1)$ cross section $\sigma_T(p,A-1)$. Thus the inclusive cross section takes the form

$$E'_{lab}\frac{d\sigma}{dp'^3_{lab}}=\frac{m_p m_A}{(2J_A+1)(2\pi)^3(Q^2)^{1/2}}\times\left(\frac{(p\cdot Q)^2-m_p^2Q^2}{(p\cdot P)^2-m_p^2m_A^2}\right)^{1/2}\times\bar{n}(p'_{lab})\sigma_T(p,A-1;\overline{T}), \qquad (3)$$

where $P=p+P_A$ is the total four-momentum. In the lab system $p\cdot P=(m_p+T_{lab})m_A$ and $Q=(m_A-E'_{lab};-\vec{p}'_{lab})$; σ_T is evaluated at the kinetic energy

$$\overline{T}=\frac{1}{2(Q^2)^{1/2}}[(p+Q)^2-(m_p+\sqrt{Q^2})^2] \qquad (4)$$

of the projectile in the Q rest frame. For $T_{lab}=0.6$ GeV and target mass of 12, $\overline{T}=0.65$ GeV, and for $T_{lab}=0.8$ GeV and target mass of 200, $\overline{T}=0.8$ GeV. $\overline{T}$ is nearly independent of T'_{lab}. The cross section $\sigma_T(p,A-1)$ should, in general depend upon the excitation of the $A-1$ system but this dependence is probably weak for the high incident proton energies of this experiment. It is thus a reasonable approximation to use the empirical total cross section for scattering of protons off nuclear ground states which yields $\sigma_T(p,A-1,\overline{T})\simeq 8.6(A-1)^{2/3}$ fm^2 (almost independent of $\overline{T}$ over our range).[4] The $A-1$ system is so near to being on shell that off-shell corrections are unnecessary.

There are two effects inherent in the $(A-1)$ nucleon-exchange mechanism which will enhance the cross section (3) over that of the single-nucleon exchange model: (i) Equation (3) is proportional to $\sigma_T(p,A-1)$ instead of $d\sigma(p,N)/d\Omega$ at $\theta=0°$, and (ii) the momentum distribution $\bar{n}$ in Eq. (3) is evaluated at a lower momentum, viz. p'_{lab} instead of at $q=p_{lab}+p'_{lab}-(2m_p\omega+\omega^2)^{1/2}$ where $\omega\simeq E(p_{lab})-E(p'_{lab})$. For example, at a beam momentum $p_{lab}=6.18$ fm^{-1} (i.e., $T_{lab}=0.6$ GeV) and a recoil momentum $p'_{lab}=2.53$ fm^{-1} (i.e., $T'_{lab}=0.1$ GeV), the effective q is approximately 3.34 fm^{-1}. This is important because, at moderately high q, any realistic single-particle momentum distribution will fall off rapidly. Furthermore, as the recoil kinetic energy T'_{lab} increases from 0 to $\approx\frac{1}{2}m_p$, which is well within the kinematic limits (e.g., for ^{12}C at $T_{lab}=0.8$ GeV, the maximal $T'_{lab}\simeq 0.51$ GeV and $p'_{lab}\simeq 0.76\,p_{lab}$), the square of the four-momentum (q^2) of the exchanged nucleon decreases from $\sim m_p^2$ to negative values. As this happens, the nucleon-exchange model gradually loses its meaning because, for such a highly virtual nucleon, the concept of a single-particle wave function becomes problematical and on-shell estimates for pN forward cross sections also are rather unreliable.

The $\bar{n}(p'_{lab})$ of Eq. (3) is related to the usual single-particle momentum distribution but differs from it in the following aspects. Whereas the single-nucleon momentum distribution $n(q)$ repre-

sents the probability that a (heavy) nucleus A at rest will virtually split into an off-shell nucleon of momentum $\vec{q}$ and a practically on-shell $A-1$ nucleon system of momentum $-\vec{q}$, our distribution $\tilde{n}$ represents a virtual splitting for which the single nucleon (recoil proton) is on shell and the $A-1$ system is off shell. We have no compelling theory which distinguishes between these two distributions, but propose two phenomenological modifications of $n(q)$ which seem reasonable. Since our theoretical $\tilde{n}(q)$,

$$\tilde{n}(q) = 2\pi \frac{E(q)}{m_p} \sum_J (2J+1)[F_l^2(q) + G_{l'}^2(q)], \tag{5}$$

with $l = J + \frac{1}{2}\omega$, $l' = J - \frac{1}{2}\omega$, $\omega = \pm 1$, and large (F_l) and small $(G_{l'})$ radial wave functions

$$F_l(q) = \int_0^\infty r F_l(r) j_l(qr) dr,$$
$$G_{l'}(q) = \int_0^\infty r G_{l'}(r) j_{l'}(qr) dr, \tag{6}$$

is obtained by summing the squares of momentum-space wave functions from a Dirac shell model, it includes pair terms[5] which here must be interpreted as the virtual splitting of the A system into a proton and a (further off-shell) $A-1$ nucleon system with a nucleon-antinucleon component. This pair contribution is quite small at low momenta but can account for as much as 90% (50% on average) of $n(q)$ at the momenta that we are considering (see Fig. 1). We may also multiply $n(q)$ by a kinematic factor

$$N^2 = \left(\frac{E_{A-1}}{E_p} \cdot \frac{E_p - m_p}{E_{A-1} - m_{A-1}} \cdot \frac{m_p^2}{m_{A-1}^2} \right)^2 \tag{7}$$

which ranges from 1 to 0.3 over our momentum range. We regard this factor N as equally uncertain, though, as it comes from studying the difference between the three-dimensional integral equations which are obtained by reducing the Bethe-Salpeter equation to three-dimensional form in two different ways: first placing the heavy particle on its mass shell while allowing the light particle to propagate off shell, and then doing the opposite. The differences in the effective interaction vertex $\langle p', A-1 | T_b | A \rangle$ were ignored in this process.

The authors of Ref. 2 use a single-particle momentum distribution $n(q)$ which is motivated by a soluble one-dimensional many-body model.[6] Although their parameters were chosen to fit the low momentum data of quasielastic electron scattering experiments,[7] it is useful to find an independent test of the momentum distribution at the high momenta of interest for this experiment.

In the absence of any other experimental or theoretical information regarding the nuclear single-particle distributions at these high momenta, we have attempted to calculate realistic $n(q)$'s using relativistic self-consistent field methods in a model[8] which leads to nuclear charge form factors in agreement with experiment out to momenta which overlap the lower range probed by backward proton production. As can be seen from Fig. 1, our distribution for protons in ^{12}C falls below that of Ref. 2 by from two to three orders of magnitude over the interesting range of momenta. This is not just an effect of the self-consistent shell model potential, as one can see from the rather similar momentum distribution generated by states in a weak Woods-Saxon shell model (used as a scalar potential in the Dirac equation) which is also shown in Fig. 1. For comparison we show in Fig. 1 the prediction of the nonrelativistic harmonic oscillator shell model which, not surprisingly, falls off even more rapidly than our two relativistic shell models. Clearly the nucleon-exchange mechanism will significantly underestimate the backward proton production cross section if used with our more realistic momentum distributions. Considering the close relationships between nuclear charge form factors and single-particle momentum distributions, it is hard to believe that our results could be wrong by several orders of magnitude over this momentum range.

Our self-consistent model yields charge form factors which are accurate out to 2.3 fm^{-1} for ^{40}Ca and 2.8 fm^{-1} for ^{208}Pb. For ^{12}C the model parameters must be corrected for the nonnegligible center of mass motion. This is done in the present work by merely scaling the coordinate space wave functions so that the experimentally observed root mean square charge radius is obtained. We thus obtain a fit to the experimental ^{12}C charge form factor[9] out to 2 fm^{-1}. From 2 to 4 fm^{-1} our charge form factor underestimates the ^{12}C data by approximately 5. One sees from Fig. 1 that the "experimental" momentum distribution obtained by solving Eq. (3) for $\tilde{n}(p'_{\text{lab}})$ and using the experimental ^{12}C backward proton cross section is also somewhat larger than our theoretical models for $\tilde{n}$ which leaves room for either the exchange of fewer than $A-1$ nucleons, or a slightly larger momentum distribution. As expected, the harmonic oscillator result falls far below the data while the scalar Woods-Saxon results are quite comparable to our self-consistent models. The wiggles present in the relativistic models are due to the fact that $\tilde{n}$ depends on only two single-particle wave functions for ^{12}C which have nodes in the momentum range of interest. One would expect the results to be smoothed by the inclusion of

some final state interaction between the backward proton and products of the p, $A-1$ reaction. The inclusion of the $\bar{N}$ components (see Fig. 1) alone tends to fill in the minima. For the Woods-Saxon well in Fig. 1, the pair terms are not so important; indeed a separate calculation shows that a momentum distribution generated by the Schrödinger equation (with the same well) is almost equivalent to that in Fig. 1.

For heavy nuclei such as ^{195}Pt, shown in Fig. 2, the self-consistent distribution lies about a factor of 10 below the data. Again, this may indicate that fewer nucleons are transferred. The self-consistent model for ^{195}Pt was obtained by summing the appropriate proton shells which resulted from the calculation of ^{208}Pb.

In summary, we have shown that realistic nuclear high momentum distributions in conjunction with a reaction mechanism involving the exchange of up to $A-1$ nucleons for the inclusive backward proton production experiments of Frankel *et al.* lead to a qualitative explanation of the data. We should also add that our mechanism is sufficiently general to apply to the backward production of deuterons and tritons as well. Further work is in progress in this area.

---

*Work supported in part by the National Science Foundation.

[1]S. Frankel *et al.*, Phys. Rev. Lett. 36, 642 (1976).

[2]R. D. Amado and R. M. Woloshyn, Phys. Rev. Lett. 36, 1435 (1976).

[3]Heavy-particle exchange is even important in large-angle elastic nucleon-nucleus interactions at intermediate energies; c.f., G. Igo, in *High-Energy Physics and Nuclear Structure*, edited by D. Nagle *et al.* (AIP, New York, 1975), p. 76.

[4]S. Barschay, C. B. Dover, and J. P. Vary, Phys. Rev. C 11, 360 (1975).

[5]L. D. Miller and H. J. Weber, Phys. Lett. 64B, 279 (1976).

[6]F. Calogero and A. Degasperis, Phys. Rev. A 11, 265 (1975); R. D. Amado and R. M. Woloshyn, Phys. Lett. 62B, 253 (1976).

[7]E. J. Moniz *et al.*, Phys. Rev. Lett. 26, 445 (1971); R. R. Whitney *et al.*, Phys. Rev. C 9, 2230 (1974).

[8]L. D. Miller and A. E. S. Green, Phys. Rev. C 5, 241 (1972); L. D. Miller, *ibid.* 14, 706 (1976).

[9]I. Sick and J. S. McCarthy, Nucl. Phys. A150, 631 (1970).